Dynamic GABAergic afferent modulation of AgRP neurons

Alastair S Garfield[1,2,9,10], **Bhavik P Shah**[1,9,10], **Christian R Burgess**[1,10], **Monica M Li**[1,10], **Chia Li**[3,4], **Jennifer S Steger**[1], **Joseph C Madara**[1], **John N Campbell**[1], **Daniel Kroeger**[5], **Thomas E Scammell**[5], **Bakhos A Tannous**[6], **Martin G Myers Jr**[7,8], **Mark L Andermann**[1], **Michael J Krashes**[3,4], and **Bradford B Lowell**[1]

[1]Division of Endocrinology, Diabetes and Metabolism, Department of Medicine, Beth Israel Deaconess Medical Center, Harvard Medical School, Boston, Massachusetts 02115, USA

[2]Centre for Integrative Physiology, Hugh Robson Building, University of Edinburgh, Edinburgh, EH8 9XD, UK

[3]Diabetes, Endocrinology and Obesity Branch, National Institute of Diabetes and Digestive and Kidney Diseases, National Institutes of Health, Bethesda, Maryland 20892, USA

[4]National Institute on Drug Abuse, National Institutes of Health, Baltimore, Maryland 21224, USA

[5]Department of Neurology, Beth Israel Deaconess Medical Center, Harvard Medical School, Boston, Massachusetts 02115, USA

[6]Department of Neurology, Massachusetts General Hospital, Harvard Medical School, Charlestown, Massachusetts 02129, USA

[7]Department of Internal Medicine, University of Michigan, Ann Arbor, MI, USA

[8]Department of Molecular and Integrative Physiology, University of Michigan, Ann Arbor, MI, USA

Abstract

Agouti-related peptide (AgRP) neurons of the arcuate nucleus of the hypothalamus (ARC) promote homeostatic feeding at times of caloric insufficiency, yet they are rapidly suppressed by food-related sensory cues prior to ingestion. Here we identify a highly selective inhibitory afferent to AgRP neurons that serves as a neural determinant of this rapid modulation. Specifically, GABAergic projections arising from the ventral compartment of the dorsomedial nucleus of the hypothalamus (vDMH) contribute to the pre-consummatory modulation of ARC^{AgRP} neurons. In a manner reciprocal to ARC^{AgRP} neurons, ARC-projecting leptin receptor (LepR)-expressing GABAergic DMH neurons exhibit rapid activation upon availability of food that additionally

Correspondence: BBL blowell@bidmc.harvard.edu; ASG alastair.garfield@pfizer.com; MJK michael.krashes@nih.gov; MLA manderma@bidmc.harvard.edu.
[9]Present address: Cardiovascular and Metabolic Diseases, Pfizer, 610 Main Street, Cambridge, MA 02139, USA.
[10]Equal contribution

reflects the relative value of the food. Thus, DMH^{LepR} neurons form part of the sensory network that relays real-time information about the nature and availability of food to dynamically modulate ARC^{AgRP} neuron activity and feeding behavior.

The sensory processing of caloric deficiency is critical to prevent starvation and ensure survival[1]. The fidelity of such need detection and response enactment is defined by an evolutionarily conserved homeostatic system that links the detection of this deficiency with the instinctual drive to consume food. ARC^{AgRP} neurons have been classically viewed as a first-order interoceptive population fundamental for this counter-regulatory response[2–4]. Indeed, increasing ARC^{AgRP} neuron activity with mounting energy deficit reflects caloric need[5] and promotes a hardwired anabolic program that drives feeding behaviour[3,6]. Experimentally, activation of ARC^{AgRP} neurons during times of caloric repletion engenders a state of artificial hunger[7] that promotes motivated food seeking[3,6] and consumption[2,3]. Remarkably however, recent investigation of the endogenous activity of ARC^{AgRP} neurons has revealed that while a high firing rate during times of caloric depletion permits overall feeding behavior, these neurons exhibit a rapid and robust decrease in activity, the onset of which is coincident with the detection/expectation of available food, prior to consumption (and maintained throughout the feeding bout)[5,7,8]. At present the functional significance of this pre-consummatory suppression remains uncertain, with numerous non-exclusive hypotheses proposed[9], including a) its role as a preparatory/predictive signal of future satiety (that prevents over-consumption and primes the celiac response for ingestion), b) its requirement for the transition from food seeking behavior to food consumption and c) its purpose as a negative teaching signal that facilitates a learning-based association between detected food items and future relief from hunger (following food ingestion)[7].

Notwithstanding this issue, the rapidity of the ARC^{AgRP} neuron response to the detection of food strongly suggests that the input responsible is neuronal in origin. As such, an important first step in understanding the nature and significance of the poly-synaptic connections that link food-related sensory input with this rapid modulatory event is the identification of the pre-synaptic population(s) that directly regulate ARC^{AgRP} neuron activity at fast timescales. Here we identify an inhibitory afferent arising from the dorsomedial nucleus of the hypothalamus (DMH) that is sufficient to robustly inhibit ARC^{AgRP} neurons and suppress homeostatic feeding. Identified by their expression of the leptin receptor (LepR) and of prodynorphin (pDYN), these pre-synaptic GABAergic DMH neurons exhibit rapid pre-consummatory activation upon detection of food, in a manner reciprocal to ARC^{AgRP} neurons. We conclude that this population plays an important role in sensory cue-mediated regulation of ARC^{AgRP} neuron activity.

Results

vDMH^{LepR} neurons are ARC^{AgRP} neuron inhibitory afferents

GABAergic modulation of ARC melanocortin neurons is well established to play a role in the regulation of energy homeostasis[10,11]. Previous monosynaptic rabies mapping[12] from genetically-defined ARC^{AgRP} neurons identified the ARC, DMH and, to a much lesser extent, the lateral hypothalamus (LH) as potential anatomic sources of pre-synaptic

input[13,14]. To validate these observations and determine their valence we employed channelrhodopsin-assisted circuit mapping (CRACM). Using a *Slc32a1(vGAT)-ires-Cre* mouse to selectively transduce putative pre-synaptic GABAergic neurons, we recorded post-synaptic currents on ARC^{AgRP} neurons (as demarked by an *Npy-GFP* transgene that labels all ARC^{AgRP} neurons[15,16]). All recorded ARC^{AgRP} neurons exhibited picrotoxin-sensitive light-evoked inhibitory post-synaptic currents (IPSCs) arising from distal DMH^{vGAT} neurons (25/25; Fig 1a, S1a) and local ARC^{vGAT} neurons (10/10; Supplementary Fig. 1b, d), but not from LH^{vGAT} neurons (0/13; Supplementary Fig. 1c, e). However, ARC-projecting DMH^{vGAT} and ARC^{vGAT} neurons were also synaptically connected to counteracting satiety-promoting ARC pro-opiomelanocortin (POMC) neurons (demarked by a *Pomc-hrGFP* transgene; Fig 1b, Supplementary Fig. 1f, g), negating the utility of the *vGAT-ires-Cre* mouse as a selective marker of inhibitory ARC^{AgRP} neuron afferents.

We subsequently identified the leptin receptor (labeled by a *Lepr-ires-Cre* mouse line) as a marker of GABAergic DMH afferents to ARC^{AgRP} neurons. Specifically, CRACM analysis demonstrated that 100% of ARC^{AgRP} neurons (31/31; Fig 1c), but only 9% of ARC^{POMC} neurons recorded (4/45; Fig 1d) and 5% of all ARC$^{non-AgRP}$ neurons (1/20; Supplementary Fig. 1h), received monosynaptic inhibitory input from DMH^{LepR} neurons (and no glutamatergic input). Furthermore, and consistent with their dense axo-somatic innervation of ARC^{AgRP} cell bodies (Fig 1e), pulsed light-evoked GABA release from DMH^{LepR}→ARC terminals was sufficient to robustly suppress ARC^{AgRP} neuron action potential firing (Fig 1f). Contrasting this selectivity, ARC^{LepR} neurons engaged 100% of recorded ARC^{AgRP} (10/10; Supplementary Fig. 1i) and ARC^{POMC} neurons (21/21; Supplementary Fig. 1j–k), while LH^{LepR} neurons did not engage either population (Supplementary Fig. 1l–m). Thus, GABAergic DMH^{LepR} neurons represent a highly preferential and potent source of pre-synaptic inhibitory input to ARC^{AgRP} neurons.

As revealed by pSTAT3 immunoreactivity (IR) GABAergic leptin-responsive DMH neurons were largely restricted to the ventral compartment (Supplementary Fig. 2a), while the glutamatergic sub-population was localized to the dorsal regions (Supplementary Fig. 2b). Consistent with this and the GABAergic nature of vDMH^{LepR}→ARC^{AgRP} neurons (Fig 1c), the majority of vDMH ARC^{AgRP} afferents are leptin-responsive (71±1.6%, n=3; Supplementary Fig. 2c–d). Together, these data suggest that the vDMH is the principle source of GABAergic DMH LepR-expressing ARC^{AgRP} neuron afferents. In addition, although as a population DMH^{LepR} neurons are widely ramifying (Supplementary Fig. 3a), the ARC-projecting axons do not collateralize to send projections to other neuroanatomical targets (Supplementary Fig. 3b–c), as demonstrated by rabies collateral mapping[17].

vDMH^{LepR}→ARC neurons are sufficient to inhibit feeding

Since direct inhibition of ARC^{AgRP} neurons suppresses food consumption[3,18] we anticipated that the *in vivo* activation of vDMH^{LepR}→ARC projections would similarly reduce food intake during times of physiological hunger, thus confirming behaviorally the inhibitory nature of the circuit. *In vivo* optogenetic stimulation of vDMH^{LepR}→ARC terminals facilitated the functional isolation of this non-collateralizing circuit from the broader DMH^{LepR} population (Fig 2a). Photostimulation of ChR2-mCherry expressing

vDMH[LepR]→ARC efferents (Supplementary Fig. 4a) prior to the initiation of consumption (10 min or 10 sec), using the same pulsed-light protocol that successfully silenced *ex vivo* ARC[AgRP] neuron firing (Fig 1f, Supplementary Fig. 4b), significantly decreased (~88%) dark-cycle food intake (Fig 2b); this was not observed in photostimulated GFP-controls (Supplementary Fig. 4c). Optogenetic activation also attenuated hyper-motivated food consumption following an overnight fast (Fig 2c), while cessation of photostimulation rapidly reestablished normal refeeding behavior (Fig 2c dashed line, Video 1). Interestingly, photostimulation of this circuit was also sufficient to halt food intake 10 seconds after the initiation of consumption following an overnight fast (Fig 2d) or during the dark cycle (Supplementary Fig. 4d). Photostimulation in the dark cycle (Supplementary Fig. 4e) or light cycle (Supplementary Fig. 4f) revealed no overt changes in locomotor activity. No changes in anxiety-like behaviors were evident in an open-field paradigm (Supplementary Fig. 4g–i). Photostimulation in the fasted state increased the time spent grooming to a level comparable to that following food intake (Supplementary Fig. 4j), consistent with an induction of satiety-like behavior[19]. Chemogenetic silencing of DMH[LepR] neurons did not increase light-cycle food consumption (Supplementary Fig. 5), indicating that this population is not required for maintaining physiological satiety. Together these data demonstrate that vDMH[LepR]→ARC neurons are sufficient, but not necessary, to robustly suppress homeostatic feeding through the inhibition of ARC[AgRP] neurons and the induction of artificial satiety.

vDMH[LepR]→ARC neurons are activated by food availability

Given these functional observations, and the inhibitory capacity of the DMH[LepR]→ARC projections, we considered whether vDMH[LepR] neurons contribute to the rapid and transient modulation of ARC[AgRP] neurons upon sensory detection of food[5,7,8]. We therefore employed *in vivo* fiber photometry to study the endogenous calcium activity of populations of vDMH[LepR] neurons during food presentation. Virally-mediated cre-dependent expression of the genetically-encoded calcium indicator GCaMP6s[20] in vDMH[LepR] neurons enabled within-subject fluorometric analysis of real-time neuronal activity.

We first assessed the population response of vDMH[LepR] cell bodies (Fig 3a) to repeated presentation of small chow pellets (14 mg). In food-restricted mice (85% of free-feeding body weight) we observed a rapid and robust increase in calcium activity upon pellet detection and approach (Fig 3b–d), as compared to a similar sized non-food object. This effect preceded the initiation of consumption (Fig 3e). The absence of a significant calcium response to a non-food item also confirms that the observed effect was not due to a startle response. In the *ad libitum* fed state, when mice were calorically replete, calcium responses to presentation of these pellets were significantly attenuated as compared to the food-restricted state (Fig 3c–d). No calcium responses to food or object presentation were evident from vDMH[LepR] neurons transduced with cre-dependent GFP (Supplementary Fig. 6a–b) or in validated 'misses' (no GCaMP6s expression in DMH; Supplementary Fig. 6c–d). Thus, vDMH[LepR] neurons exhibit a pre-consummatory response that is similar in nature but opposite in sign to AgRP neurons[8] - a decrease in activity upon food presentation the magnitude of which correlates with the animal's hunger state.

Larger chow pellets (500 mg) also elicited a calcium response that exhibited energy-state dependence (Fig 3f–g), however this response was of greater magnitude than that observed with small pellets (Fig 3h), suggesting that vDMH^{LepR} neuron activity conveys information not only about the presence but the nature of discovered food items. ARC^{AgRP} neurons exhibit exaggerated pre-consummatory suppression upon the presentation of chocolate – a highly palatable food that is more calorically dense and rewarding (compared to chow)[8]. As predicted, presentation of chocolate fragments (approximately 14 mg) elicited an increase in GCaMP6 fluorescence in DMH^{LepR} cell bodies. In contrast to chow presentation, responses to chocolate presentation did not vary across fasted vs. fed states (Fig 3i–j), possibly due to sustained food-seeking for chocolate vs. chow pellets in the *ad libitum* fed state. Furthermore, and as observed of ARC^{AgRP} neurons[7], vDMH^{LepR} neuron fluorometric responses to chocolate were significantly greater than to similar sized chow pellets (Fig 3k). Thus, the pre-consummatory activation of vDMH^{LepR} neurons is potentiated by the nutritive value of detected food, in a manner that reflects both food quantity and quality.

To isolate the vDMH^{LepR}→ARC projecting neurons from the broader DMH^{LepR} population, we assessed calcium activity specifically in vDMH^{LepR}→ARC axons (Fig 4a). As observed in population activity from vDMH^{LepR} cell bodies, axonal calcium activity in food-restricted mice rapidly increased upon small chow pellet presentation (Fig 4b–d) prior to consumption (Fig 4e–g), but not in reaction to a non-food object or in the *ad libitum* fed state. Larger chow pellets elicited larger calcium responses compared to small pellets (Fig 4h and Supplementary Fig. 7a–b), similar to responses in vDMH^{LepR} cell bodies. The vDMH^{LepR}→ARC axon responses were larger to presentation of chocolate *vs.* small pellets, and did not depend on hunger state (Fig 4i and Supplementary Fig. 7c–d). In sum, vDMH^{LepR}→ARC neurons respond to availability of food in a manner opposite to that of ARC^{AgRP} neurons, relaying real-time sensory information regarding the availability and quality of food.

A subset of vDMH^{LepR}→ARC neurons are dynorphinergic

In light of the heterogeneity of DMH^{LepR} neurons[21–23], we sought to further specify the neurochemical identity of GABAergic vDMH^{LepR}→ARC^{AgRP} afferents. Recent analysis of hypothalamic LepR neurons has indicated that a subset of those in the DMH express the inhibitory neuropeptide pDYN[24]. Quantitative PCR analysis of individual manually-isolated vDMH^{LepR} neurons revealed that 14/25 (56%) of those expressing *Slc32a1* (*vGAT*) also expressed *Pdyn* (Supplementary Fig. 8a–b). Consistent with the location of vDMH^{LepR}→ARC^{AgRP} neurons (Supplementary Fig. 2) the preponderance of leptin-responsive vDMH^{pDYN} neurons (as defined by pSTAT3 immunoreactivity) were within the vDMH (Supplementary Fig. 8c–e and Ref 18). Furthermore, projection profiling from DMH^{pDYN} neurons identified the mediobasal ARC as their only long-range target (Supplementary Fig. 8f–h).

CRACM analysis demonstrated that almost all recorded ARC^{AgRP} neurons (20/21; Fig 5a) but no ARC$^{non-AgRP}$ neurons (Supplementary Fig. 8i; including ARC^{POMC} neurons, Fig 5b) received direct GABAergic input from vDMH^{pDYN} neurons. vDMH^{pDYN}→ARC^{AgRP} IPSCs were of smaller amplitude compared to those derived from vDMH^{LepR} afferents

(Supplementary Fig. 8j) which led to less effective light-evoked inhibition of ARC^{AgRP} neuron spiking (Supplementary Fig. 8k). This suggests that $vDMH^{pDYN}$ neurons are only a proportion of the total GABAergic $vDMH^{LepR}{\rightarrow}ARC^{AgRP}$ population. *In vivo* optogenetic activation of $vDMH^{pDYN}{\rightarrow}ARC$ terminals suppressed food consumption during the dark cycle (Fig 5c) and following an overnight fast (Fig 5d). The magnitude of feeding suppression was less than that observed of the $vDMH^{LepR}{\rightarrow}ARC$ circuit (Fig 2), especially during a post-fast refeed, likely reflecting the weaker inhibitory potency of this circuit.

Subsequent *in vivo* GCaMP6s photometry demonstrated that $vDMH^{pDYN}$ neurons showed similar functional properties to $vDMH^{LepR}$ neurons and $DMH^{LepR}{\rightarrow}ARC$ axons. Small pellets presented to hungry mice elicited a significant increase in calcium activity, prior to consumption, which was not observed upon detection of a non-food item or in *ad libitum* fed mice (Fig 5e–g). Calcium responses in food-restricted mice were potentiated by presentation of larger chow pellets (Fig 5h–j) and chocolate (Fig 5k–m), with chocolate responses being independent of energy-state. Together, these data suggest that $vDMH^{pDYN}$ neurons represent a sub-population of GABAergic $vDMH^{LepR}{\rightarrow}ARC^{AgRP}$ afferents.

Discussion

Using a combination of *in vivo* techniques for the manipulation and monitoring of genetically-defined neuronal populations we identify a source of inhibitory input to ARC^{AgRP} neurons that contributes to their rapid sensory regulation[5,7,8]. This population of GABAergic $vDMH^{LepR}/vDMH^{pDYN}$ neurons exhibits a highly circumscribed efferent field within the ventromedial ARC with dense peri-somatic innervation of ARC^{AgRP} somata. As such, they provide a highly selective inhibitory input sufficient to robustly silence ARC^{AgRP} neuron action potential firing and supress homeostatic feeding, when photostimulated. It is important to note that the complete inhibition of ARC^{AgRP} neurons by way of the optogenetic activation of GABAergic $vDMH^{LepR}{\rightarrow}ARC$ terminals (Fig 1f) represents a supra-physiological paradigm that exceeds the level of suppression induced by food availability[5]. Thus, while providing behavioural validation for the nature of the circuit such optogenetic manipulation does not speak to the physiological role of ARC^{AgRP} neurons (or $vDMH^{LepR}{\rightarrow}ARC$ neurons) in the regulation of homeostatic feeding. Indeed, as observed by others[22,23], DMH^{LepR} neurons were not necessary for the maintenance of homeostatic satiety, indicating that they are not a source of tonic ARC^{AgRP} neuron inhibition contributing to feeding suppression during times of caloric sufficiency. This circuit may however offer a highly tractable experimental approach for the real-time temporal control of ARC^{AgRP} neurons.

Recent investigations of the endogenous activity of ARC^{AgRP} neurons has revealed their pre-consummatory suppression upon food presentation/expectation[5,7,8]. The rapidity of this response strongly suggests that it is synaptically, rather than hormonally, mediated. Indeed, that all ARC^{AgRP} neurons recorded received GABAergic $vDMH^{LepR/pDYN}$ input is consistent with the majority of ARC^{AgRP} neurons exhibiting pre-consummatory suppression[5,7]. Thus, in light of the specificity and potency of the $vDMH^{LepR}{\rightarrow}ARC$ circuit we asked whether it contributed to the dynamic modulation of ARC^{AgRP} neurons during food discovery. Strikingly, reciprocal to ARC^{AgRP} neurons, $vDMH^{LepR}$ cell bodies and

$vDMH^{LepR} \rightarrow ARC$ axons exhibited rapid and reproducible pre-consummatory activation upon food detection. Chow presentation elicited fluorescent responses with both cue- and energy state-dependency, indicating some level of neural gating upstream of these neurons is important for attributing salience to the sensory input, in a manner that considers the animal's broader external and internal environment. Furthermore, as observed of ARC^{AgRP} neurons[8], the magnitude of calcium responses in $vDMH^{LepR}$ neurons and their ARC projections increased with presentation of more palatable food. Thus, in the fasted state, the potentiation of the $vDMH^{LepR} \rightarrow ARC$ response to increased nutritive content (both quality and quantity) may signal the greater value of the food item as a source of relief from hunger. However, as reflected by $vDMH^{LepR} \rightarrow ARC$ neuron activity (and feeding behavior), food quantity loses, but food quality retains incentive value in the calorically replete state, possibly suggesting a switch in value processing from the homeostatic to the hedonic in the absence of a physiological hunger drive.

Other populations of neuronal afferents also contribute to the sensory regulation of ARC^{AgRP} neurons. Indeed, although $vDMH^{LepR}$ neuron activity peaked upon food approach prior to consumption, we observed a decay in the peak amplitude of the calcium response before the termination of feeding. This contrasts with the sustained reduction in ARC^{AgRP} neuron activity throughout consumption[5,7,8] and may suggest that additional inputs are important for prolonged ARC^{AgRP} neuron suppression. This could include inhibition via other GABAergic afferents, such as ARC^{vGAT} neurons, and/or dis-facilitation via removal of tonic excitatory inputs – such as those arising from the PVH[13]. To this latter possibility, it is interesting to note that ARC^{AgRP} neurons do not express the kappa-opioid receptor (KOR)[25] (and data not shown), raising the possibility that any DYN released from $vDMH^{LepR/pDYN}$ neurons may act pre-synaptically to inhibit a KOR-expressing excitatory ARC^{AgRP} neuron afferents. The kinetics of pre-synaptic neuropeptide action would define a slower onset but longer-lasting modulation of ARC^{AgRP} neurons and potentially explain their sustained suppression during consumption. This model is also consistent with slow recovery in ARC^{AgRP} neuron activity when presented food is subsequently removed prior to or during the consummatory phase[7,8].

The significance of LepR expression on GABAergic $vDMH^{LepR/pDYN} \rightarrow ARC$ neurons also remains to be determined. In acute electrophysiological slices leptin depolarizes GABAergic $vDMH^{LepR}$ neurons (data not shown). This raises the possibility that low leptin levels, by decreasing the basal activity of these neurons, may increase their dynamic range and facilitate their response to food related sensory cues. Alternatively, it is possible that LepR signaling at these neurons is involved in a slower transcriptional modulation, potentially related to synaptic restructuring. In this way, LepR signaling at $vDMH^{LepR} \rightarrow ARC^{AgRP}$ neurons may concern longer-term regulation reflecting the chronic nutritional state, such as might underlie maladapted associations between sensory cues and feeding behavior in obesity or eating disorders. Real-time monitoring of $vDMH^{LepR}$ neuron activity in diet-induced or genetically obese mice will prove informative in this regard.

As a population, DMH^{LepR} neurons have been implicated in a number of physiologies, including autonomic regulation of energy expenditure and cardiovascular tone[22,23,21]. Although the specific networks underlying these functions are yet to be defined, it is likely

that they are independent of the vDMH^{LepR}→ARC^{AgRP} circuit. DMH^{LepR} neurons that regulate energy expenditure are glutamatergic and located in the dorsal DMH[22,26] and thus spatially and neurochemically distinct from GABAergic vDMH^{LepR}→ARC^{AgRP} neurons. Furthermore, the thermogenic effect of DMH^{LepR} neurons has been demonstrated to be melanocortin independent[21]. For a number of reasons it is also unlikely that the vDMH^{LepR}→ARC^{AgRP} circuit is involved in cardiovascular control. Firstly, DMH mediated regulation of blood pressure is predicted to proceed via more direct projections to pre-autonomic neurons in the RVLM[27]. Secondly, leptin-mediated or chemogenetic activation of DMH^{LepR} neurons only influences blood pressure after 3 days of chronic simulation[23,28], inconsistent with the acute modulatory function of vDMH^{LepR}→ARC^{AgRP} neurons. Thirdly, no feeding suppression was observed during chemogenetically-induced hypotension[23], as would be expected of activation of the vDMH^{LepR}→ARC^{AgRP} circuit. It is therefore likely that vDMH^{LepR}→ARC neurons represent a functionally specific sub-population involved in transitory sensory modulation of ARC^{AgRP} neurons. Of note, LepR-expressing vDMH^{pDYN} neurons are distinct from the non-LepR expressing cDMH^{pDYN} neurons implicated in the attenuation of food consumption during intense feeding bouts[29].

The rapid pre-consummatory inhibition of ARC^{AgRP} neurons and their sustained suppression during consumption represents a fascinating new aspect of their physiological function[5,7,8], although the significance of this phenomenon for feeding behaviour remains controversial. Our data now expand an understanding of the nature and source of this modulation. Specifically, we identify GABAergic vDMH$^{LepR/pDYN}$ neurons as a potent inhibitory afferent to ARC^{AgRP} neurons that, like their post-synaptic target, are rapidly regulated by food detection. As expected, the directionality of this modulation is reciprocal to ARC^{AgRP} neurons but occurs on a comparable timescale. Furthermore, like ARC^{AgRP} neurons, vDMH$^{LepR/pDYN}$ neuron activity reflects not only the presence, but also the quality of the food item. These observations strongly support the hypothesis that vDMH$^{LepR/pDYN}$ neurons are a physiologically relevant source of inhibitory input to ARC^{AgRP} neurons and provide an entry point into the upstream circuitry that underlies rapid evaluation of sensory food cues during homeostatic feeding.

Material and methods

Animals

Slc32a1(vGAT)-ires-Cre[11], *Lepr-ires-Cre[30]*, *Pdyn-ires-Cre[13]*, *Npy-hrGFP[15]*, *Pomc-hrGFP[31]*, *Rosa26-loxSTOPlox-L10-GFP[13]* mice were generated and maintained as previously described. All mice are on a mixed background. All animal care and experimental procedures were approved by the National Institute of Health and Beth Israel Deaconess Medical Center Institutional Animal Care and Use Committee. Mice were housed at 22–24 °C with a 12 h light:12 h dark cycle with standard mouse chow (Teklad F6 Rodent Diet 8664; 4.05 kcal g^{-1}, 3.3 kcal g^{-1} metabolizable energy, 12.5% kcal from fat; Harlan Teklad) and water provided *ad libitum*, unless otherwise stated. All diets were provided as pellets. For all behavioral studies male mice between 6–10 weeks were used. For electrophysiological studies male mice between 4–8 weeks were used.

Brain tissue preparation

Mice were terminally anesthetised with chloral hydrate (Sigma Aldrich) and transcardially perfused with phosphate-buffered saline (PBS) followed by 10% neutral buffered formalin (Fisher Scientific). Brains were extracted, cryoprotected in 20% sucrose, and sectioned coronally on a freezing sliding microtome (Leica Biosystems) at 30 μm and collected in four equal series.

Immunohistochemistry

Brain sections were washed in 0.1 M phosphate-buffered saline pH 7.4, blocked in 3% normal donkey serum/0.25% Triton X-100 in PBS for 1 hour at room temperature and then incubated overnight at room temperature in blocking solution containing primary antiserum (rabbit anti-dsRed, Clonetech (#632496) 1:1000; chicken anti-GFP, Life Technologies (#A10262). The next morning sections were extensively washed in PBS and then incubated in Alexa fluorophore secondary antibody (Molecular Probes, 1:1000) for 2 h at room temperature. After several washes in PBS, sections were mounted onto gelatin-coated slides and fluorescent images were captured with Olympus VS120 slide scanner microscope. All primary antibodies used are validated for species and application (1DegreeBio and Antibody Registry).

pSTAT3 immunohistochemistry

Mice were injected with 5 mg/kg recombinant leptin two hours prior to perfusion (as above). Brain sections were washed in 0.1 M phosphate-buffered saline pH 7.4 followed by incubation in 5% NaOH and 0.3% H_2O_2 for 2 min, then with 0.3% glycine (10 min), and finally with 0.03% SDS (10 min), all made up in PBS. Sections were blocked in 3% normal donkey serum/0.25% Triton X-100 in PBS for 1 hour at room temperature and then incubated overnight at room temperature in blocking solution containing 1/250 rabbit anti-pSTAT3 (Cell Signalling, #9145) and 1/1000 chicken anti-GFP (Life Technologies, #A10262). The next morning sections were extensively washed in PBS and then incubated in 1/250 donkey anti-rabbit 594 (Molecular Probes, R37119) and 1/1000 donkey anti-chicken 488 (Jackson ImmunoResearch, 703-545-155) for 2 h at room temperature. After several washes in PBS, sections were mounted onto gelatin-coated slides and fluorescent images were captured with Olympus VS120 slide scanner microscope.

Single cell quantitative PCR

DMH was acutely dissected from adult *LepR-ires-Cre::L10-GFP* mice (n=2), then enzymatically dissociated and manually sorted for GFP+ cells as described previously[32]. Isolated GFP positive cells and negative control samples (cell-picking buffer) were concurrently processed into cDNA libraries using Smart-Seq2[33], except that the amplified cDNA was eluted in 30 μl volumes. Gene expression was analyzed by probe-based qPCR on a 7500 Fast Real-Time PCR System (Applied Biosystems) using Brilliant II qPCR Low ROX Master Mix (Agilent Technologies) according to the manufacturer's instructions. Each 20 μl qPCR reaction contained 2 μl of eluted cDNA and 1 μl of a custom primer/probe set (sequences below; 1:1 ratio of primer:probe; default FAM/ZEN modifications; IDT). Cells showing relatively little to no expression of *Gfp*, *Actb*, or *Slc32a1* were excluded from

further analysis. Remaining cells were analyzed for expression of *Pdyn*. A heatmap of Ct values was generated using GenePattern software (Broad Institute), with a "global" color scale for across-gene comparisons. Note that in order to include cells for which no signal was detected in 40 cycles of qPCR, a "pseudocount" of 40 was entered as the Ct. Primers (5′→3′): *Actb* (L, AAAAGGGAGGCCTCAGACCTGG; R, TCACCCTCCCAAAAGCCACC; probe, GCCCTGAGTCCACCCCGGGG); *Gfp* (L, ATCTGCACCACCGGCAAGCT; R, ATCTGCACCACCGGCAAGCT; probe, CGTGCCCTGGCCCACCCTCG); *Slc32a1* (L, ACGAGCACACCACACGCACA; R, ATTTCGGGCGGGCGACTTCA; probe, GGCCCCGTTTGCCTGCCGGT); *Pdyn* (L, AGGATGGGGGATCAGGTAGGGCA; R, CACCTTGAACTGACGCCGCA; probe, GGGGGGCTTCCTGCGGCGCAT).

Viral injections

Stereotaxic injections were performed as previously described. Mice were anaesthetised with xylazine (5 mg per kg) and ketamine (75 mg per kg) diluted in saline (350 mg per kg) and placed into a stereotaxic apparatus (KOPF Model 963 or Stoelting). For postoperative care, mice were injected intraperitoneally with meloxicam (5 mg/kg). After exposing the skull via small incision, a small hole was drilled for injection. A pulled-glass pipette with 20–40 mm tip diameter was inserted into the brain and virus was injected by an air pressure system. A micromanipulator (Grass Technologies, Model S48 Stimulator) was used to control injection speed at 25 nl min^{-1} and the pipette was withdrawn 5 min after injection. For electrophysiology and *in vivo* optogenetic experiments, AAV8-hSyn-DIO-ChR2(H134R)-mCherry (University of North Carolina Vector Core; titer 1.3×10^{12} genome copies per ml) was injected into the ARC (15–50 nl, AP: −1.50 mm, DV: −5.80 mm, ML: +/−0.20 mm from bregma), DMH (50 nl, AP: −1.80 mm, DV: −5.2 mm, ML: +/−0.3 mm from bregma), LH (50–100 nl, AP: −1.50 mm, DV: −5.00 mm, ML: +/−1.00 mm from bregma). For electrophysiology and *in vivo* chemogenetic experiments, AAV8-hSyn-DIO-hM4Di-mCherry (University of North Carolina Vector Core; titer 1.7×10^{12} genome copies per ml) were bilaterally injected into the DMH (15–40 nl, coordinates as above). For *ex vivo* and *in vivo* calcium imaging experiments, AAV1-hSyn-DIO-GCaMP6(s) (University of Pennsylvania Vector Core) was injected into the DMH (50 nl, coordinates as above). Mice were given a minimum of 2 weeks recovery and 1 week acclimation before being used in any experiments.

Electrophysiology

To prepare brain slices for electrophysiological recordings, brains were removed from anesthetized mice (4–8 weeks old) and immediately submerged in ice-cold, carbogen-saturated (95% O_2, 5% CO_2) high sucrose solution (238 mM sucrose, 26 mM $NaHCO_3$, 2.5 mM KCl, 1.0 mM NaH_2PO_4, 5.0 mM $MgCl_2$, 10.0 mM $CaCl_2$, 11 mM glucose). Then, 300-μM thick coronal sections were cut with a Leica VT1000S Vibratome and incubated in oxygenated aCSF (126 mM NaCl, 21.4 mM $NaHCO_3$, 2.5 mM KCl, 1.2 mM NaH_2PO_4, 1.2 mM $MgCl_2$, 2.4 mM $CaCl_2$, 10 mM glucose) at 34 °C for 30 minThen, slices were maintained and recorded at room temperature (20–24°C). For most voltage clamp recordings intracellular solution contained the following (in mM): 140 CsCl, 1 BAPTA, 10 HEPES, 5 $MgCl_2$, 5 Mg-ATP, 0.3 Na_2GTP, and 10 lidocaine *N-ethyl* bromide (QX-314), pH 7.35 and

290 mOsm. The intracellular solution for current clamp recordings contained the following (in mM): 128 K gluconate, 10 KCl, 10 HEPES, 1 EGTA, 1 $MgCl_2$, 0.3 CaCl2, 5 Na2ATP, 0.3 NaGTP, adjusted to pH 7.3 with KOH.

Light-evoked IPSCs and EPSCs during CRACM studies[34,35] were recorded in the whole cell voltage clamp mode, with membrane potential clamped at −60 mV. In a subset of voltage clamp CRACM experiments it was necessary to detect light-evoked GABAergic synaptic currents in ChR2-mCherry expressing neurons (Supplementary Fig. 2d, h, i). As such, to negate the movement of monovalent cations, a Cs^+ based low Cl^- internal solution was used (129 mM $CsMeSO_4$, 16 mM CsCl, 8mM NaCl, 10 mM HEPES, 0.25 mM EGTA, 3 mM Mg-ATP, 0.3 mM Na_2GTP) and light-evoked IPSCs recorded at ~0 mV. All recordings were made using multiclamp 700B amplifier, and data was filtered at 2 kHz and digitized at 10 kHz. To photostimulate Channelrhodopsin2-positive fibers, a laser or LED light source (473 nm; Opto Engine LLC; Thorlabs) was used. The blue light was focused on to the back aperture of the microscope objective, producing a wide-field exposure around the recorded cell of 1 mW. The light power at the specimen was measured using an optical power meter PM100D (ThorLabs). The light output is controlled by a programmable pulse stimulator, Master-8 (AMPI Co. Israel) and the pClamp 10.2 software (AXON Instruments). Photostimulation-evoked EPSCs/IPSCs detection protocol constitutes four blue light laser pulses (pulse duration - 2 ms) administered 1 second apart, repeating for a total of 30 sweeps. When recording light-evoked changes in membrane potential in AgRP neurons, current (~5 pA) was injected into cells to maintain continuous action potential firing.

Number of animals used per study (all male): $DMH^{vGAT} \rightarrow ARC^{AgRP}$ n=2; $DMH^{vGAT} \rightarrow ARC^{POMC}$ n=3; $ARC^{vGAT} \rightarrow ARC^{AgRP}$ n=4; $ARC^{vGAT} \rightarrow ARC^{POMC}$ n=5; $LH^{vGAT} \rightarrow ARC^{AgRP}$ n=2; $LH^{vGAT} \rightarrow ARC^{POMC}$ n=2; $DMH^{LepR} \rightarrow ARC^{AgRP}$ n=3; $DMH^{LepR} \rightarrow ARC^{POMC}$ n=6; $ARC^{LepR} \rightarrow ARC^{AgRP}$ n=2; $ARC^{LepR} \rightarrow ARC^{POMC}$ n=4; $LH^{LepR} \rightarrow ARC^{AgRP}$ n=1; $LH^{LepR} \rightarrow ARC^{POMC}$ n=3. $DMH^{pDYN} \rightarrow ARC^{AgRP}$ n=4; $DMH^{pDYN} \rightarrow ARC^{POMC}$ n=2.

Optic fiber implantation

Optic fiber implantations were performed during the same surgery as viral injection (above). For optogenetic photostimulation of DMH→ARC terminals, ceramic ferrule optical fibers (200 μm diameter core, BFH37-200 Multimode, NA 0.37; Thor Labs) were implanted bilaterally over the ARC (AP: −1.55 mm, DV: (R) −5.75 mm and (L) − 5.50 mm, ML: (R) +0.3 mm and (L at 20°) −2.40 mm from bregma). For DMH^{LepR} and DMH^{pDYN} cell body calcium photometry a metal ferrule optic fiber (200 μm diameter core; BFH37-200 Multimode; NA 0.37; Thor Labs) was implanted unilaterally over the vDMH (AP: −1.80 mm, DV: −5.0 mm, ML: +0.3 mm from bregma). For DMH^{LepR}→ARC axon calcium photometry a metal ferrule optic fiber (400 μm diameter core; BFH37-400 Multimode; NA 0.37; Thor Labs) was implanted unilaterally over the ARC (AP: −1.55 mm, DV: −5.8 mm, ML: (at 2°) −0.49 mm from bregma). Fibers were fixed to the skull using dental acrylic and mice were allowed 2 weeks for recovery before acclimatisation to home cages customized for optogenetic stimulation or photometry recording (12 h light/dark cycle starting at 6am) for 1 week. After the completion of the experiments, mice were perfused and the

approximate locations of fiber tips were identified based on the coordinates of Franklin and Paxinos.[36]

Food intake studies

Food intake studies on chow were performed as previously described. All animals were singly housed for at least 2.5 weeks following surgery and handled for 10 consecutive days before the assay to reduce stress response. Studies were conducted in a home-cage environment with *ad libitum* food access. A full trial consisted of assessing food intake from the study subjects after they received injections of saline or pseudo-photostimulation on day-1 and 1 mg/kg CNO or photostimulation on day-2. Animals received a week 'off' between trials before another trial was initiated. The food intake data from all days were then averaged and combined for analysis. Mice with 'missed' injections, incomplete 'hits' or expression outside the area of interest were excluded from analysis after post hoc examination of mCherry expression. In this way, all food intake measurements were randomised and blind to the experimenter.

Dark-cycle feeding studies were conducted between 6:00pm to 9:00pm and intake was monitored for three hours. For post-fast refeed studies, animals were fasted overnight at 5:00pm and food returned the following morning at 9:00am. Food intake was monitored for five hours after photostimulation. Light-cycle feeding studies were conducted between 9:00am to 12:00pm and intake was monitored for three hours.

In vivo optogenetic studies

In vivo photostimulation was conducted as previously described[32]. Fiber optic cables (1.25 m long, 200 μm diameter, 0.37 NA; Doric Lenses) were firmly attached to the implanted fiber optic cannulae with zirconia sleeves (Doric Lenses). Animals were stimulated with blue light (473 nm) at 10 Hz, 5 ms pulses for 5 sec with a 1 sec recovery period (laser off) during stimulation trains to avoid neuronal transmitter depletion and tissue heating. Photostimulation was provided using a waveform generator (PCGU100; Valleman Instruments or Arduino electronics platform) that provided TTL input to a blue light laser (Laserglow). We adjusted the power of the laser such that the light power exiting the fiber optic cable was at least 10 mW. Using an online light transmission calculator for brain tissue http://web.stanford.edu/group/dlab/cgi-bin/graph/chart.php we estimated the light power at the ARC to be 18.35 mW/mm^2. Mice were tethered to the patch cords at least 1 hour prior to the commencement of any experiment.

To test the sufficiency of DMH^{LepR}→ARC neurons for satiety mice were tested under two conditions of physiological hunger, at the onset of the dark cycle and refeeding following an overnight fast.. For dark cycle feeding analysis mice with *ad libitum* access to food were photostimulated for 10 min prior to the onset of the dark cycle (which serves as a natural cue for the initiation of feeding behaviour) and photostimulation maintained for the duration of the study. For post-fast refeeding analysis mice were photostimulated 10 min prior to food presentation (which serves as an experimental cue for the initiation of feeding behaviour) and photostimulation maintained for the duration of the study. In the explicit case of the 'ON

(After) group' in Figure 2D, mice were allowed to consume freely for 5 min and then photostimulated for the duration of the experiment.

Behavioural profiling

Open field testing was conducted in *ad libitum* fed mice during the light cycle. Mice were placed in a large arena (40 cm × 40 cm) in which they were allowed to freely explore for 20 min. Trials were recorded via a CCD camera interfaced with Ethovision software for offline analysis of distance moved, time spent at the edge and center of the arena. Animals were run in a counter-balanced order of laser-on versus laser-off to avoid acclimation.

For assessment of homecage behaviour mice were compared in the fasted state with photostimulation and *ad libitum* fed state during the light cycle in the absence of food. 10 minute trials were recorded via a CCD camera interfaced with Ethovision software for offline analysis of time spent grooming and total distance moved. Animals were run in a counter-balanced order of laser-on versus laser-off to avoid acclimation. Locomotor activity during the dark cycle was also assessed in ad libitum fed mice with and without laser stimulation, in the presence of food.

In vivo fiber photometry

All photometery experiments were conducted as within-subject, with animals tested in both the fed and fasted state. Studies were conducted in the animal's homecage. Beginning two weeks post-surgery (details above) mice were food restricted to 85–90% of starting body weight. Over this one week period mice were acclimated to the chow pellets (both small and large) used in subsequent photometry experiments. Mice were habituated to the paradigm for 1–2 days prior to the first recording day. *In vivo* fiber photometry was conducted as previously described[8]. Fiber optic cables (1 m long, metal ferrule, 400 μm diameter; Doric Lenses) were firmly attached to the implanted fiber optic cannulae with zirconia sleeves (Doric Lenses). Laser light (473 nm) was focused on the opposite end of the fiber optic cable such that a light intensity of 0.1–0.2mW entered the brain; light intensity was kept constant across sessions for each mouse. Emission light was passed through a dichroic mirror (Di02-R488-25×36, Semrock) and GFP emission filter (FF03-525/50-25, Semrock), before being focused onto a sensitive photodetector (2151, Newport). The signal was passed through a low-pass filter (50Hz) and digitized with a National Instruments data acquisition card and collected using a custom MATLAB script. Photobleaching over the course of each 30 min run was negligible, most likely due to the very low laser power used for excitation (0.1 mW) and the short duration of each run. Although we continued to observe clear responses to food presentation at the end of each run (in the food restricted state) we did note average 37% decrease between first and last responses. It is possible that minor photobleaching contributed to this effect, though it was likely predominantly due to reduced novelty of food and some level of caloric repletion.

Each 30 minute session consisted of 4–6 trials of chow (14 mg pellets) or chocolate (14 mg pellets) and 4–6 trials of a similar sized non-food object (bedding), in an alternating fashion. Large pellets (500 mg) required up to 15 minutes to consume and therefore only had 1–2 presentations per a run, with alternating non-food item presentation. Only one food type was

used in a given run. Up to 4 runs were performed in a single day for each mouse and mice were run multiple days, with large pellet and chocolate runs never preceding small pellet runs. All trials across days (14mg: 12 ± 1 presentations per mouse; 500 mg: 6 ± 0.7; chocolate: 7 ± 0.6) were pooled to calculate mean response to food/object in each mouse. After fasted runs mice were given *ad libitum* access to chow for 5–7 days and the above studies repeated in the fed state. Within run responses to the same food stimulus showed a trend towards a decrease in response magnitude (decreasing by 37% from the first to the last instance of food availability; data not shown) this may reflect decreasing novelty or increasing satiety (as mice had consumed food throughout the run prior to the last instance of food presentation).

For data analysis, fluorescent traces were down-sampled to 1Hz. dF/F $(F − F0)/F0$; where F0 was the 20 sec prior to food presentation) was calculated for each presentation of food. Small pellets (per 14mg pellet 0.01 Kcal from protein, 0.007 Kcal from fat and 0.03 Kcal from carbohydrate; Bio-Serv). Large pellets (per 500 mg pellet 0.38 Kcal from protein, 0.25 Kcal from fat and 1.18 Kcal from carbohydrate; Bio-Serv) or 14 mg chocolate (Hershey's) or control (cob bedding of size comparable to food). In a subset of mice both time of food availability and the moment when the mouse first made contact with the food item were recorded. For analysis differentiating approach from consumption, the 10s prior to food availability was compared to the time between food availability and consumption and to the 10s following contact with the food item.

Monosynaptic rabies mapping

AgRP-ires-Cre::RABVgp4-TVA mice expressing the avian TVA receptor and rabies glycoprotein selectively in ARC^{AgRP} neurons were injected with SADΔG–EGFP (EnvA) rabies (Salk Gene Transfer Targeting and Therapeutics Core; titer 7.5×10^8 infectious units per ml) unilaterally into the ARC (n=3). Animals were allowed 6 days for retrograde transport of rabies virus and EGFP expression before perfusion and tissue collection. Sites of afferent input to ARC^{AgRP} neurons were assessed by the presence of EnvA-EGFP positive neurons and the slides imaged on an Olympus VS120 slide scanner microscope.

Rabies collateral mapping[17]

Three weeks after unilateral injection of AAV8-EFIα-DIO-TVA-mCherry (University of North Carolina Vector Core; titer 1.1×10^{12} genomes copies per ml) into the DMH of *LepR-ires-Cre* mice, SADΔG–EGFP (EnvA) rabies (Massachusetts General Hospital Vector Core; titer 10^7 infectious units per ml) was unilaterally injected into the ARC. Animals were allowed 6 days for retrograde transport of rabies virus and EGFP transgene expression before perfusion and tissue collection. Comprehensive examination of SADΔG–EGFP (EnvA) axonal and retrograde transductions were obtained using 10–15 confocal images of DMH^{LepR}→ARC boutons along the neuraxis using an Zeiss LSM-510 confocal microscope.

Statistical analysis

Statistical analyses were performed using Origin Pro 8.6 and Prism 6.0 (GraphPad) software. Details of statistical tests employed can be found in the relevant figure legends and supplementary methods checklist. Power analyses were calculated to estimate sample size

using statistical conventions for 80% power, assuming a standard deviation of change of 1.0, a difference between the means of 1.5-fold and alpha level of 0.05. In all statistical tests normal distribution and equal variance was established. The data presented met the assumptions of the statistical test employed. No randomisation of animals was conducted since all behavioral tests were within-subject comparisons. Exclusion criteria for experimental animals were a) sickness or death during the testing period or b) if histological validation of the injection site demonstrated an absence of reporter gene expression. These criteria were established prior to data collection. N-numbers represent final number of healthy/validated animals.

Data availability

The data that support the findings of this study are available from the corresponding author upon request.

Supplementary Material

Refer to Web version on PubMed Central for supplementary material.

Acknowledgments

References

1. Sternson SM, Nicholas Betley J, Cao ZF. Neural circuits and motivational processes for hunger. Curr Opin Neurobiol. 2013; 23:353–360. [PubMed: 23648085]

2. Aponte Y, Atasoy D, Sternson SM. AGRP neurons are sufficient to orchestrate feeding behavior rapidly and without training. Nat Neurosci. 2011; 14:351–355. [PubMed: 21209617]

3. Krashes MJ, et al. Rapid, reversible activation of AgRP neurons drives feeding behavior in mice. J Clin Invest. 2011; 121:1424–1428. [PubMed: 21364278]

4. Luquet S, Perez FA, Hnasko TS, Palmiter RD. NPY/AgRP neurons are essential for feeding in adult mice but can be ablated in neonates. Science. 2005; 310:683–685. [PubMed: 16254186]

5. Mandelblat-Cerf Y, et al. Arcuate hypothalamic AgRP and putative POMC neurons show opposite changes in spiking across multiple timescales. Elife. 2015; 4

6. Dietrich MO, Zimmer MR, Bober J, Horvath TL. Hypothalamic Agrp neurons drive stereotypic behaviors beyond feeding. Cell. 2015; 160:1222–1232. [PubMed: 25748653]

7. Betley JN, et al. Neurons for hunger and thirst transmit a negative-valence teaching signal. Nature. 2015; 521:180–185. [PubMed: 25915020]

8. Chen Y, Lin YC, Kuo TW, Knight ZA. Sensory detection of food rapidly modulates arcuate feeding circuits. Cell. 2015; 160:829–841. [PubMed: 25703096]

9. Chen Y, Knight ZA. Making sense of the sensory regulation of hunger neurons. Bioessays. 2016; 38:316–324. [PubMed: 26898524]

10. Pinto S, et al. Rapid rewiring of arcuate nucleus feeding circuits by leptin. Science. 2004; 304:110–115. [PubMed: 15064421]

11. Vong L, et al. Leptin action on GABAergic neurons prevents obesity and reduces inhibitory tone to POMC neurons. Neuron. 2011; 71:142–154. [PubMed: 21745644]

12. Wickersham IR, Finke S, Conzelmann KK, Callaway EM. Retrograde neuronal tracing with a deletion-mutant rabies virus. Nat Methods. 2007; 4:47–49. [PubMed: 17179932]

13. Krashes MJ, et al. An excitatory paraventricular nucleus to AgRP neuron circuit that drives hunger. Nature. 2014; 507:238–242. [PubMed: 24487620]

14. Wang D, et al. Whole-brain mapping of the direct inputs and axonal projections of POMC and AgRP neurons. Front Neuroanat. 2015; 9:40. [PubMed: 25870542]

15. van den Pol AN, et al. Neuromedin B and gastrin-releasing peptide excite arcuate nucleus neuropeptide Y neurons in a novel transgenic mouse expressing strong Renilla green fluorescent protein in NPY neurons. J Neurosci. 2009; 29:4622–4639. [PubMed: 19357287]

16. Hahn TM, Breininger JF, Baskin DG, Schwartz MW. Coexpression of Agrp and NPY in fasting-activated hypothalamic neurons. Nat Neurosci. 1998; 1:271–272. [PubMed: 10195157]

17. Betley JN, Cao ZF, Ritola KD, Sternson SM. Parallel, redundant circuit organization for homeostatic control of feeding behavior. Cell. 2013; 155:1337–1350. [PubMed: 24315102]

18. Vardy E, et al. A New DREADD Facilitates the Multiplexed Chemogenetic Interrogation of Behavior. Neuron. 2015; 86:936–946. [PubMed: 25937170]

19. Rodgers RJ, Holch P, Tallett AJ. Behavioural satiety sequence (BSS): separating wheat from chaff in the behavioural pharmacology of appetite. Pharmacol Biochem Behav. 2010; 97:3–14. [PubMed: 20214921]

20. Chen TW, et al. Ultrasensitive fluorescent proteins for imaging neuronal activity. Nature. 2013; 499:295–300. [PubMed: 23868258]

21. Enriori PJ, Sinnayah P, Simonds SE, Garcia Rudaz C, Cowley MA. Leptin action in the dorsomedial hypothalamus increases sympathetic tone to brown adipose tissue in spite of systemic leptin resistance. J Neurosci. 2011; 31:12189–12197. [PubMed: 21865462]

22. Rezai-Zadeh K, et al. Leptin receptor neurons in the dorsomedial hypothalamus are key regulators of energy expenditure and body weight, but not food intake. Mol Metab. 2014; 3:681–693. [PubMed: 25352997]

23. Simonds SE, et al. Leptin mediates the increase in blood pressure associated with obesity. Cell. 2014; 159:1404–1416. [PubMed: 25480301]

24. Allison MB, et al. TRAP-seq defines markers for novel populations of hypothalamic and brainstem LepRb neurons. Mol Metab. 2015; 4:299–309. [PubMed: 25830093]

25. Henry FE, Sugino K, Tozer A, Branco T, Sternson SM. Cell type-specific transcriptomics of hypothalamic energy-sensing neuron responses to weight-loss. Elife. 2015; 4

26. Knight ZA, et al. Molecular profiling of activated neurons by phosphorylated ribosome capture. Cell. 2012; 151:1126–1137. [PubMed: 23178128]

27. Cao WH, Morrison SF. Glutamate receptors in the raphe pallidus mediate brown adipose tissue thermogenesis evoked by activation of dorsomedial hypothalamic neurons. Neuropharmacology. 2006; 51:426–437. [PubMed: 16733059]

28. Fontes MA, Tagawa T, Polson JW, Cavanagh SJ, Dampney RA. Descending pathways mediating cardiovascular response from dorsomedial hypothalamic nucleus. Am J Physiol Heart Circ Physiol. 2001; 280:H2891–2901. [PubMed: 11356650]

29. Shek EW, Brands MW, Hall JE. Chronic leptin infusion increases arterial pressure. Hypertension. 1998; 31:409–414. [PubMed: 9453337]

30. Leshan RL, Bjornholm M, Munzberg H, Myers MG Jr. Leptin receptor signaling and action in the central nervous system. Obesity (Silver Spring). 2006; 14(Suppl 5):208S–212S. [PubMed: 17021368]

31. Parton LE, et al. Glucose sensing by POMC neurons regulates glucose homeostasis and is impaired in obesity. Nature. 2007; 449:228–232. [PubMed: 17728716]

32. Garfield AS, et al. A neural basis for melanocortin-4 receptor-regulated appetite. Nat Neurosci. 2015; 18:863–871. [PubMed: 25915476]

33. Picelli S, et al. Full-length RNA-seq from single cells using Smart-seq2. Nat Protoc. 2014; 9:171–181. [PubMed: 24385147]

34. Petreanu L, Huber D, Sobczyk A, Svoboda K. Channelrhodopsin-2-assisted circuit mapping of long-range callosal projections. Nat Neurosci. 2007; 10:663–668. [PubMed: 17435752]

35. Atasoy D, Aponte Y, Su HH, Sternson SM. A FLEX switch targets Channelrhodopsin-2 to multiple cell types for imaging and long-range circuit mapping. J Neurosci. 2008; 28:7025–7030. [PubMed: 18614669]

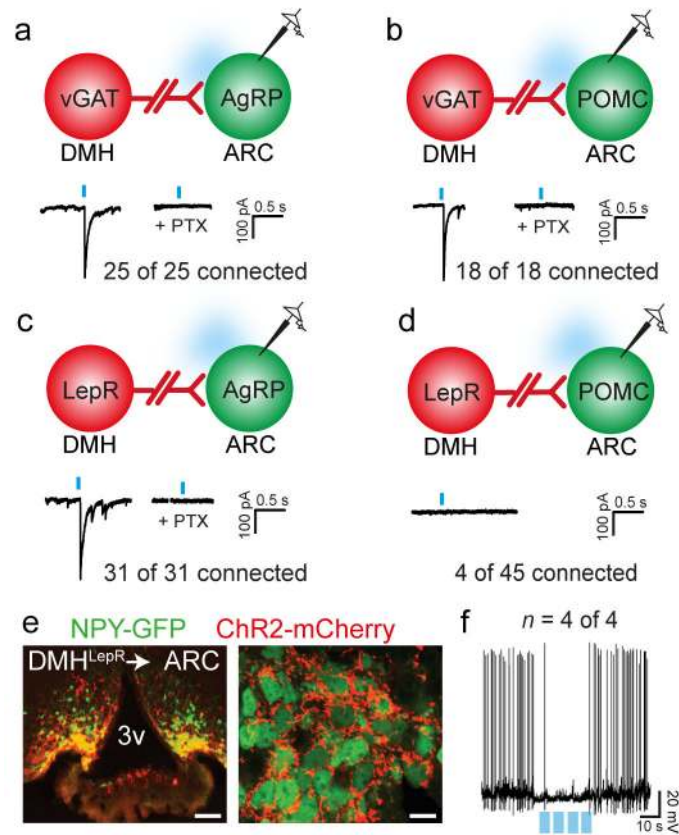36. Franklin, BJaPG. The Mouse Brain in Stereotaxic Coordinates. Academic Press, Elsevier; New York, NY: 2008.

Figure 1. DMH$^{\text{LepR}}$ neurons are a potent source of GABAergic input to ARC$^{\text{AgRP}}$ neurons
(**a–b**), DMH$^{\text{vGAT}}$ neurons provide monosynaptic inhibitory input to 100% of ARC$^{\text{AgRP}}$ neurons (a) and ARC$^{\text{POMC}}$ neurons recorded (b). (**c–d**), DMH$^{\text{LepR}}$ neurons provide selective monosynaptic input to 100% of ARC$^{\text{AgRP}}$ (c) but only 9% of ARC$^{\text{POMC}}$ neurons recorded (d). (**e**), DMH$^{\text{LepR}}$→ARC neurons provide dense axo-somatic innervation of ARC$^{\text{AgRP}}$ neurons. (**f**), Photostimulation of DMH$^{\text{LepR}}$→ARC terminals is sufficient to inhibit ARC$^{\text{AgRP}}$ action potential firing. Abbreviations, 3v, third ventricle; PTX, picrotoxin. Scale bar in panel e, 100 μm and f, 25 μm.
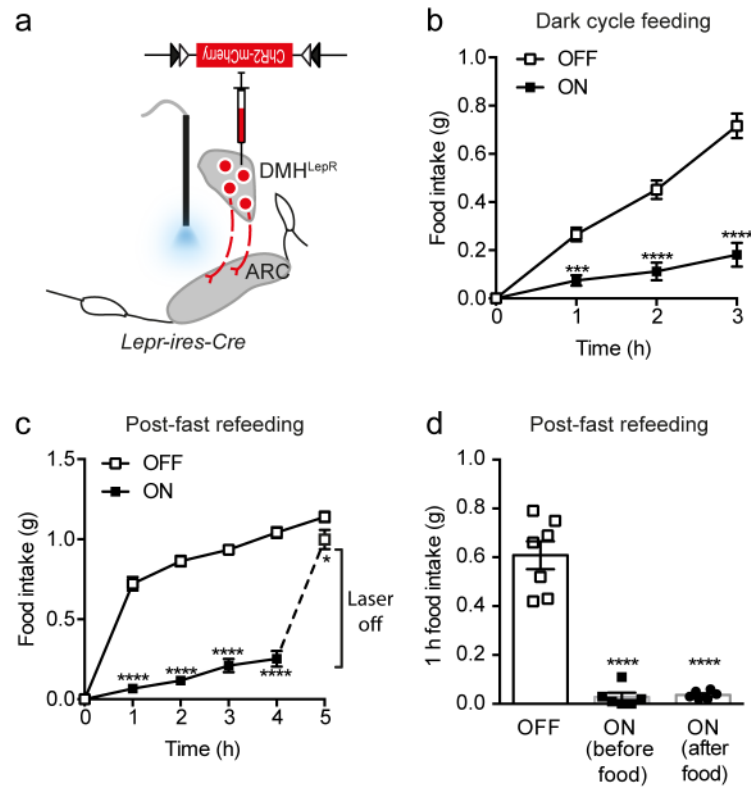
Figure 2. DMH^{LepR}→ARC neurons are sufficient to inhibit homeostatic feeding
(**a–c**), *in vivo* optogenetic stimulation of DMH^{LepR}→ARC terminals (a) significantly reduced food consumption during the dark-cycle (b; n=12, repeated measures ANOVA, main effect of treatment ($F_{(1,44)}$=171.10, p<0.0001), main effect of time ($F_{(3,44)}$=48.48, p<0.0001) and interaction ($F_{(3,44)}$=30.95, p<0.0001) and following an overnight fast (c; n=15, repeated measures ANOVA, main effect of treatment ($F_{(1,84)}$=569.90, p<0.0001), main effect of time ($F_{(3,84)}$=226.50, p<0.0001) and interaction ($F_{(3,84)}$=43.74, p<0.0001). (**d**), photostimulation of DMH^{LepR}→ARC terminals in a post-fast refeed paradigm was sufficient to inhibit food intake when applied before or after food consumption had begun (n=7 (off) and 6 (on), ANOVA, $F_{(2,16)}$=6.73, p=0.0074). Abbreviations, Before, before food presentation; After, after the initiation of consumption. All data presented as mean±SEM; post-hoc p-values *p<0.05; ***p<0.001; ****P<0.0001.

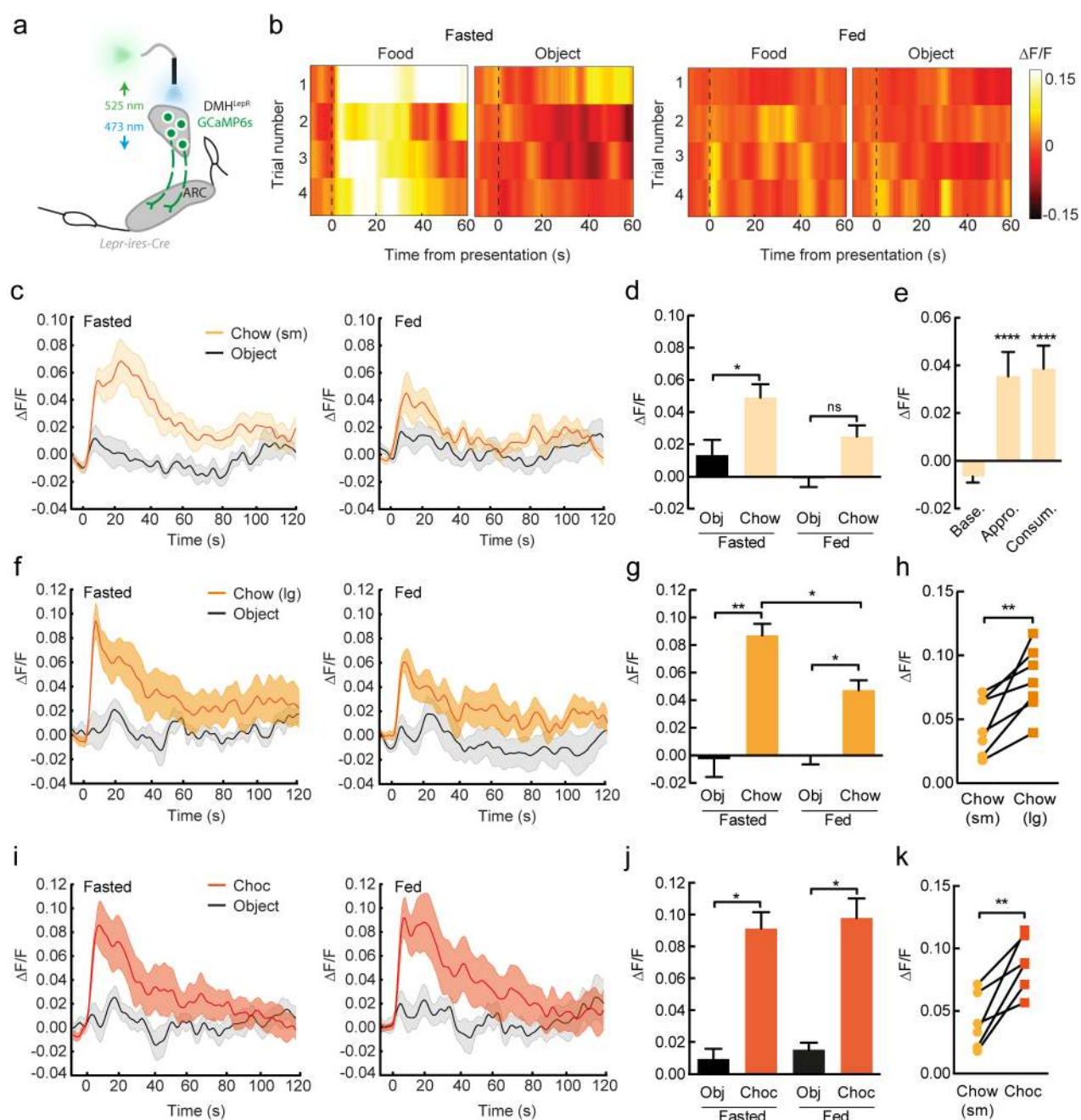**Figure 3. DMH^LepR neurons are rapidly activated upon sensory detection of food**
(**a**)**,** the real-time activity of DMH^LepR cell bodies was determined using *in vivo* fiber
photometry. (**b–d**), DMH^LepR neurons were rapidly activated upon presentation of a small
chow pellet (t=0), compared to a non-food object, in a energy-state dependent manner (b,
individual trials in one representative mouse on one day in the calorie restricted and *ad
libitum* fed state; c, mean effects from all mice across time, n=6; d, mean response from 0–
10s post food presentation, repeated measures ANOVA, $F_{(5,15)}$=7.2, p=0.02). **e**, responses of
DMH^LepR to small pellet availability occurred prior to the initiation of consumption and was
not increased further once consumption began (n=15; repeated measures ANOVA,

$F_{(14,28)}$=12.16, p=0.0002). (**f–g**), DMH^{LepR} neurons were rapidly activated upon presentation of a large chow pellet, compared to a non-food object, in a energy-state dependent manner (f, mean effects from all mice across time, n=6; d, mean response from 0–10s post food presentation, repeated measures ANOVA, $F_{(5,15)}$=24.15, p=0.0001). (**h**), response of DMH^{LepR} neurons to large chow pellets was potentiated compared to that elicited by small chow pellets in the same mouse (n=7; paired t-test, $t_{(6)}$=3.88, p=0.0081). (**i–j**), presentation of chocolate activated DMH^{LepR} neurons, compared to a non-food object, and was comparable to responses in *ad libitum* chow-fed mice (i, mean effects from all mice across time, n=5; j, mean response from 0–10s post food presentation, repeated measures ANOVA, $F_{(4,12)}$=24.21, p=0.0003). (**k**), responses to chocolate were increased compared to chow (n=6, paired t-test, $t_{(5)}$=4.58, p=0.006). All data presented as mean±SEM; post-hoc p-values *p<0.05; **p<0.01; ****P<0.0001. Abbreviations, ΔF/F, fractional change in fluorescence.

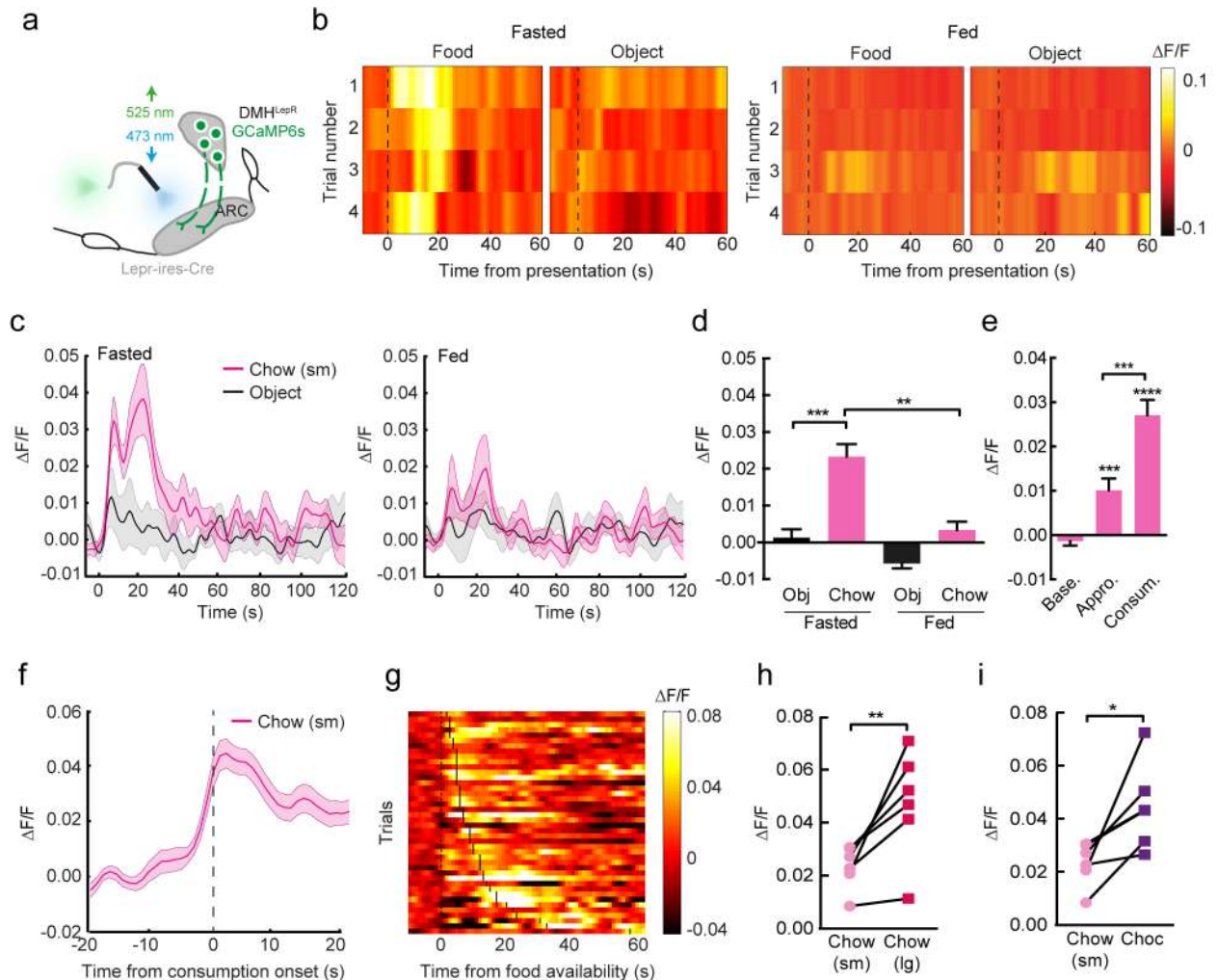**Figure 4. DMH$^{\mathrm{LepR}}$→ARC axons are rapidly activated upon sensory detection of food**
(**a**), the real-time activity of DMH$^{\mathrm{LepR}}$→ARC axons was determined using *in vivo* fiber photometry. (**b–d**), DMH$^{\mathrm{LepR}}$→ARC axons were rapidly activated upon presentation of a small chow pellet (t=0), compared to a non-food object, in a energy-state dependent manner (b, individual trials in one representative mouse on one day in the calorie restricted and ad libitum fed state; c, mean effects from all mice across time, n=6; d, mean response from 0–10s post food presentation, repeated measures ANOVA, $F_{(5,15)}$=36.08, p<0.0001). (**e**), activation of DMH$^{\mathrm{LepR}}$→ARC axons to small pellet availability occurred prior to the initiation of consumption (n=36; repeated measures ANOVA, $F_{(35,70)}$=35.30, p<0.0001). (**f–g**), Mean responses to small pellet presentation aligned to onset of consumption (f) and individual trial responses aligned to food availability (g; onset of consumption denoted with vertical black bar on each trial) demonstrating activity rising prior to consumption. (**h–i**), calcium response of DMH$^{\mathrm{LepR}}$→ARC axons to large chow pellets (h; n=6; paired t-test, $t_{(6)}$=3.61, p=0.015) and chocolate (i; n=6; paired t-test, $t_{(6)}$=3.13, p=0.026) were potentiated compared to that elicited by small chow pellets in the same mouse. All data presented as

mean±SEM; post-hoc p-values *p<0.05; **p<0.01; ***p<0.001; ****P<0.0001. Abbreviations, ΔF/F, fractional change in fluorescence.
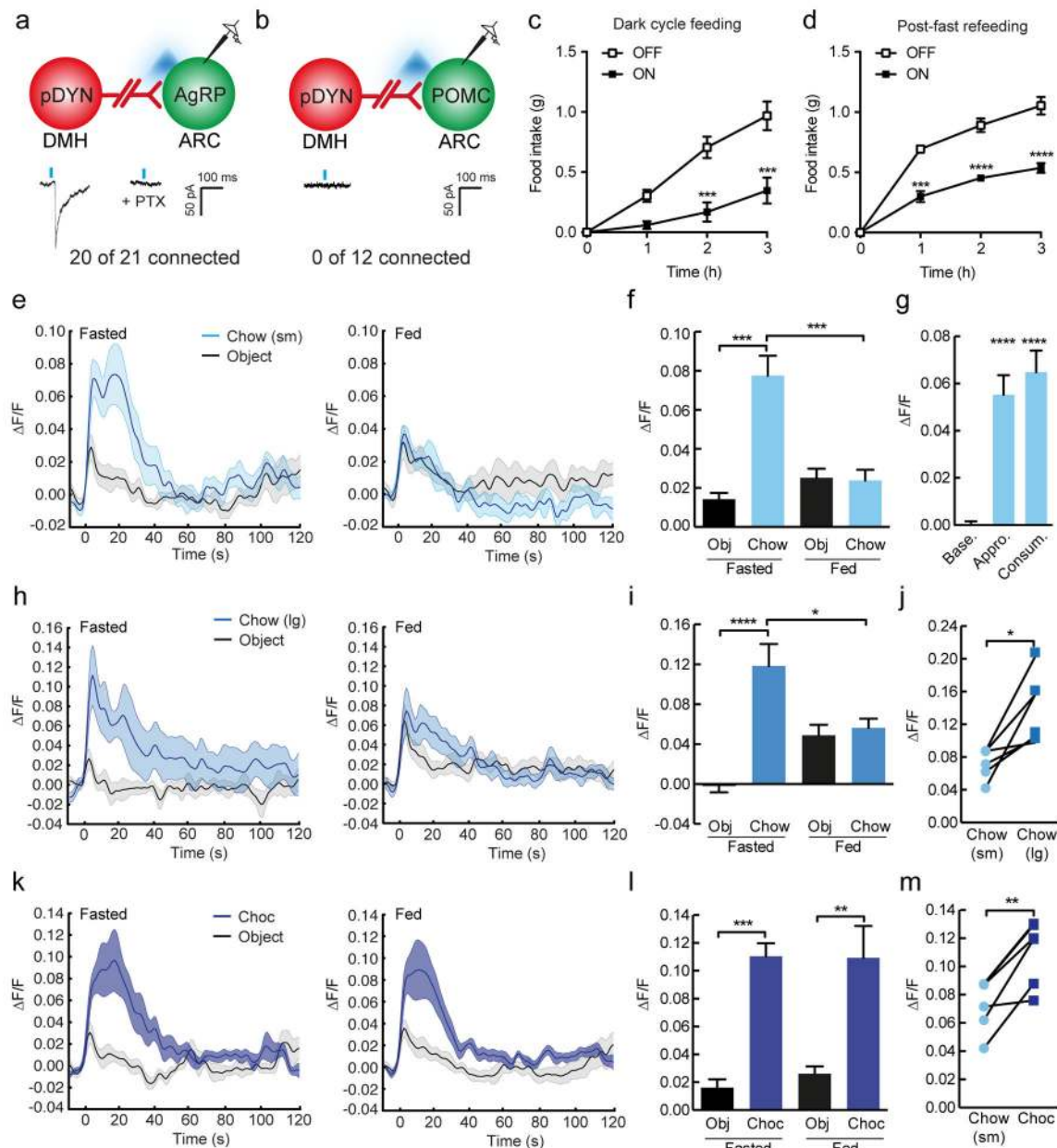
Figure 5. DMH^{pDYN} neurons are a subset of GABAergic DMH^{LepR}→ARC neurons

(**a–b**), DMH^{pDYN} neurons (red) provide monosynaptic inhibitory input to 95% of ARC^{AgRP} (a; 20/21 connected) neurons recorded but not ARC^{POMC} neurons (b; 0/12 connected). (**c–d**), *in vivo* optogenetic stimulation of DMH^{pDYN}→ARC terminals significantly reduced food consumption during the dark-cycle (c; n=3, repeated measures ANOVA, main effect of treatment ($F_{(1,8)}$=77.14, p<0.0001), main effect of time ($F_{(3,8)}$=21.49, p=0.0003) and interaction ($F_{(3,8)}$=12.69, p=0.002) and following an overnight fast (d; n=3, repeated measures ANOVA, main effect of treatment ($F_{(1,8)}$=193.60, p<0.0001), main effect of time ($F_{(3,8)}$=111.90, p<0.0001) and interaction ($F_{(3,8)}$=22.63, p=0.0003). (**e–f**), *in vivo* fiber photometry demonstrated that DMH^{pDYN} neurons were rapidly activated upon presentation

of a small chow pellet (t=0), compared to a non-food object, in a energy-state dependent manner (e, mean effects from all mice across time, n=5–6; f, mean response from 0–10s post food presentation, one-way ANOVA, $F_{(3,18)}=19.56$, $p<0.0001$). (**g**), activation of DMH^{pDYN} to small pellet availability occurred prior to the initiation of consumption and was not increased further once consumption began (n=44; repeated measures ANOVA, $F_{(43,86)}=40.61$, $p<0.0001$). (**h–i**), DMH^{pDYN} neurons were rapidly activated upon presentation of a large chow pellet, compared to a non-food object, in a energy-state dependent manner (h, mean effects from all mice across time, n=5–6; i, mean response from 0–10s post food presentation, one-way ANOVA, $F_{(3,18)}=13.43$, $p<0.0001$). (**j**), calcium response of DMH^{pDYN} neurons to large chow pellets was potentiated compared to that elicited by small chow pellets in the same mouse (n=6; paired t-test, $t_{(5)}=3.56$, $p=0.016$). (**k–l**), presentation of chocolate activated DMH^{pDYN} neurons, compared to a non-food object, and was comparable to *ad libitum* chow-fed mice (k, mean effects from all mice across time, n=5–6; l, mean response from 0–10s post food presentation, one-way ANOVA, $F_{(3,18)}=18.03$, $p<0.0001$). (**m**), DMH^{pDYN} neuron calcium responses to chocolate were increased compared to chow (n=6, paired t-test, $t_{(5)}=5.09$, $p=0.0038$). All data presented as mean±SEM; post-hoc p-values: *$p<0.05$; **$p<0.01$; ***$p<0.001$; ****$P<0.0001$. Abbreviations, ΔF/F, fractional change in fluorescence.